論文 97-8-3-06

랜덤 표면으로부터 산란되는 전자파의 편파적 해석

Polarimetric Analysis of the Electromagnetic Waves Scattered from Random Surfaces-Full Wave Solutions

이 범 선

Bom-Son Lee

요 약

본 논문에서는 랜덤적 성질을 갖는 2차 표면으로부터 산란되는 전자파를 4×4 Mueller 행렬 요소를 이용하여 특성화 한다. 이러한 요소 계산에는 Full wave solution이 사용되는데 이 해를 이용한 계산 결과는 1차 표면에 대하여 실험 결과 및 모멘트 법을 이용한 결과와 잘 일치하는 것으로 이미 발표된 바 있다. Mueller 행렬 요소는 Like-Pol과 Cross-Pol RCS에 대한 정보를 포함할 뿐 아니라 입사파와 산란파의 수직.수평 편파 위상차에 대한 정보도 포함하고 있기 때문에 목표물로부터 산란되는 전자파를 완전하게 특성화 한다. 이 논문의 계산 결과들은 능동 원격탐사나 RCS 분야에 유용하리라 생각한다.

Abstract

In this work, the electromagnetic waves scattered from 2-dimensional random rough surfaces are characterized by the 4×4 Mueller matrix elements. The full wave solutions are used to compute these elements. The results of the full wave solutions for 1-dimensional random rough surfaces were shown to agree well with those of the experiment and the method of moments. The Mueller matrix elements are related to the like and cross polarized radar cross sections as well as to the relative phase of the vertically and horizontally polarized waves. The 4×4 Mueller matrix elements completely characterize electromagnetic scattering from target. The computed results of this paper can be useful to the field of active remote sensing or RCS.

I. Introduction

The scattering of electromagnetic waves by rough surfaces is challenging to many researchers in diversified areas such as EM theory, light scattering, remote sensing, and so on. There have been numerous efforts to obtain the solution through decades of research works. Rice's small perturbation solution[1] was obtained based on the assumption that the root mean square surface height is very small and of the same order of smallness as the surface slopes. When the surface radius

「이 연구는 1996년도 경희대학교 교비지원에 의한 결과임.」

경희대학교 전파공학과 (Dept. of Radio Science & Engineering, Kyunghee Univ.)

· 논 문 번 호 : 970311-015
· 수정완료일자 : 1997년 5월 6일

of curvature and correlation length are large compared with the free space wavelength, Beckman's physical optics solution[2] is considered to be a good approximation. If, in addition to the conditions for the physical optics solution, the root mean square surface height is very large, the limiting form of the physical optics solution becomes the geometrical optics solution. In an effort to exploit the advantages of both the small perturbation and physical optics solution, the two-scale model was introduced[3]. However, the results based on this model depend on a particular choice of the spectrum division. Recently the integral equation was solved numerically using the method of moments[4][5]. The main disadvantage of this solution is that it takes too much time. Until recently, these numerical solutions had been practically restricted to one-dimensional rough surfaces.

The full wave approach[6]~[9] is used here to compute the 4×4 Mueller matrix elements which completely characterize the electromagnetic waves scattered from the targets(in this case, 2-dimesional random rough surfaces).

The polarization state of an electromagnetic wave can be described in terms of the four Stokes parameters which are measurable. The 4×4 Mueller matrix relates the 4×1 incident Stokes vector to the 4×1 scattered Stokes vector. It completely characterizes the waves scattered from rough surfaces. If the Mueller matrix elements for a particular rough surface are known, the Stokes vector of the scattered waves is readily obtained for arbitrary excitations. The elements of a Mueller matrix are dependent on rough surface parameters and medium characteristics above and below the rough surface. They are also dependent on the incident and scattered angles. The main motivation of this work is to polarimetrically characterize the waves scattered from random rough surfaces through the Mueller matrix elements.

The Mueller matrix elements are computed for the backscatter direction as a function of the incident angle. They are also plotted as a function of the root mean square surface height and the correlation length for a fixed incident angle. Their relationships to the ellipsometric parameters are also considered.

Ⅱ. Formulation of the Problems

2-1 General Features of Jones Vector and Stokes Vector

Let E_1 and E_2 be the two complex electric field components given by

$$E_1 = |E_1|\exp(i\phi_1) \tag{1}$$

$$E_2 = |E_2|\exp(i\phi_2) \tag{2}$$

The Jones vectors are usually defined as

$$E^k = \begin{bmatrix} E_1^k \\ E_2^k \end{bmatrix} = \begin{bmatrix} E^{Vk} \\ E^{Hk} \end{bmatrix} = \begin{bmatrix} E_\theta^k \\ E_\phi^k \end{bmatrix} \tag{3}$$

where

$k=i, f.$

E^i denotes the Jones vector for incident fields and E^f denotes the Jones vector for the scattered fields. The electric fields E_1 and E_2 are orthogonal to each other. They may be E_x

and E_y in the Cartesian coordinate system or they may be E_θ (or E^v) and E_ϕ (or E^h) in the spherical coordinate system. We also define the Stokes vector

$$G = \begin{bmatrix} G_0 \\ G_1 \\ G_2 \\ G_3 \end{bmatrix}$$

$$= \begin{bmatrix} <|E_1|^2 + |E_2|^2> \\ <|E_1|^2 - |E_2|^2> \\ 2\,\mathrm{Re} < E_1 E_2^* > \\ 2\,\mathrm{Im} < E_1 E_2^* > \end{bmatrix} \tag{4}$$

$$= \begin{bmatrix} <|E_1|^2 + |E_2|^2> \\ <|E_1|^2 - |E_2|^2> \\ 2<|E_1||E_2|\cos\phi> \\ 2<|E_1||E_2|\sin\phi> \end{bmatrix}$$

where

$$\phi = \phi_1 - \phi_2 \tag{5}$$

and E_1, E_2 and ϕ are random in general. The symbol $< >$ is the averaging operator.

For the monochromatic wave with constant field amplitude and constant phase difference ϕ,

$$G = \begin{bmatrix} G_0 \\ G_1 \\ G_2 \\ G_3 \end{bmatrix}$$

$$= \begin{bmatrix} |E_1|^2 + |E_2|^2 \\ |E_1|^2 - |E_2|^2 \\ 2|E_1||E_2|\cos\phi \\ 2|E_1||E_2|\sin\phi \end{bmatrix} \tag{6}$$

In this case of completely polarized waves, it can readily be shown that $G_0^2 = G_1^2 + G_2^2 + G_3^2$.

Another extreme case is that of an unpolarized wave (or natural light). For natural light, $G_1=G_2=G_3=0$, because ϕ is completely random and thus $<\cos\phi>$ and $<\sin\phi>$ go to zero.

However, in general, $G_0^2 \geq G_1^2+G_2^2+G_3^2 \geq 0$. The degree of polarization is defined as

$$V = \frac{G_1^2+G_2^2+G_3^2}{G_0^2} \quad (0 \leq V \leq 1) \tag{7}$$

If $V = 0.7$, it means that 70 % of the waves are polarized and 30 % of the them are unpolarized. The typical polarization states are shown in Table 1. The Stokes vectors in this table have been normalized.

Table 1. Typical polarization states and their Stokes vectors

Polarization state	Stokes vector
Vertically polarized wave	$[1 \quad 1 \quad 0 \quad 0]^T$
Horizontally polarized wave	$[1 \quad -1 \quad 0 \quad 0]^T$
Linear +45° polarized	$[1 \quad 0 \quad 1 \quad 0]^T$
Linear −45° polarized	$[1 \quad 0 \quad -1 \quad 0]^T$
Right circularly polarized	$[1 \quad 0 \quad 0 \quad 1]^T$
Left circularly polarized	$[1 \quad 0 \quad 0 \quad -1]^T$
Unpolarized (Natural light)	$[1 \quad 0 \quad 0 \quad 0]^T$

Sometimes the Stokes vector G is modified as follows since the first two elements are associated with the scattering cross sections for vertically and horizontally polarized waves

$$G_m=\begin{bmatrix} G_{m0} \\ G_{m1} \\ G_{m2} \\ G_{m3} \end{bmatrix} = \begin{bmatrix} <|E_1|^2> \\ <|E_2|^2> \\ 2\mathrm{Re}<E_1E_2^*> \\ 2\mathrm{Im}<E_1E_2^*> \end{bmatrix} \tag{8}$$

Table 2 shows the typical polarization states and their modified Stokes vectors of which elements have been normalized.

Table 2. Typical polarization states and their Stokes vectors

Polarization state	Modified stokes vector
Vertically polarized wave	$[1 \quad 0 \quad 0 \quad 0]^T$
Horizontally polarized wave	$[0 \quad 1 \quad 0 \quad 0]^T$
Linear +45° polarized	$[1/2 \quad 1/2 \quad 1 \quad 0]^T$
Linear −45° polarized	$[1/2 \quad 1/2 \quad -1 \quad 0]^T$
Right circularly polarized	$[1/2 \quad 1/2 \quad 0 \quad 1]^T$
Left circularly polarized	$[1/2 \quad 1/2 \quad 0 \quad -1]^T$
Unpolarized (Natural light)	$[1/2 \quad 1/2 \quad 0 \quad 0]^T$

Using the full wave approach, the diffusely scattered fields from two-dimensional rough surfaces are given by [9],[10]

$$\begin{bmatrix} E_1^f \\ E_2^f \end{bmatrix} = S \begin{bmatrix} E_1^i \\ E_2^i \end{bmatrix} = G_0 S_0 \begin{bmatrix} E_1^i \\ E_2^i \end{bmatrix} = G_0 \begin{bmatrix} S_0^{VV} & S_0^{VH} \\ S_0^{HV} & S_0^{HH} \end{bmatrix} \begin{bmatrix} E_1^i \\ E_2^i \end{bmatrix}$$

$$= G_0 \iint \begin{bmatrix} D^{VV} & D^{VH} \\ D^{HV} & D^{HH} \end{bmatrix} [\exp(i\bar{v}\cdot\bar{r}_s) - \exp(i\bar{v}\cdot\bar{r}_t)]$$

$$dx_s dz_s \begin{bmatrix} E_1^i \\ E_2^i \end{bmatrix} \tag{9a}$$

where

$$G_0 = \frac{k_0^2 \exp(-ik_0 r)}{2\pi i v_y r} \tag{9b}$$

$$\bar{v} = \bar{k}_0^f - \bar{k}_0^i = v_x \bar{a}_x + v_y \bar{a}_y + v_z \bar{a}_z \tag{9c}$$

$$\bar{k}_0^f = k_0 (\sin\theta_0^f \cos\phi^f \bar{a}_x + \cos\theta_0^f \bar{a}_y + \sin\theta_0^f \sin\phi^f \bar{a}_z) \tag{9d}$$

$$\bar{k}_0^i = k_0 (\sin\theta_0^i \cos\phi^i \bar{a}_x - \cos\theta_0^i \bar{a}_y + \sin\theta_0^i \sin\phi^i \bar{a}_z) \tag{9e}$$

$$\bar{r}_s = x_s \bar{a}_x + y_s \bar{a}_y + z_s \bar{a}_z \tag{9f}$$

$$\bar{r}_t = x_s \bar{a}_x + z_s \bar{a}_z \tag{9g}$$

D^{PQ} $(P,Q = V, H)$ are the elements of the 2×2 rough surface differential scattering coefficient matrix $D(\bar{k}^f, \bar{k}^i)$[11] which accounts for the slopes of the rough surface (h_x, h_z), and $S_0^{PQ}(P, Q = V, H)$ are the elements of the scattering matrix $S_0(\bar{k}^f, \bar{k}^i)$ which relate the scattered fields from the whole radar footprint to the incident fields. S_0^{PQ} depends on the incident and scatter angles, rough surface parameters, and electromagnetic characteristics of the medium above and below the rough surface. In order to make the scattering matrix $S_0(\bar{k}^f, \bar{k}^i)$ independent of the distance r from the target to the receiver, G_0 has been factored out from S. $\bar{r}_s$ is the position vector from the origin to the position on the rough surface and $\bar{r}_t$ is the projection of $\bar{r}_s$ on the mean plane $y_s=0$.

2-2 Coherency vector and Mueller matrix

For the derivation of the Mueller matrix, we also define the coherency vector J^k $(k = i, f)$ as follows[12]

$$J^k = \langle E^k \times E^{k*} \rangle = \left\langle \begin{bmatrix} E_1^k \\ E_2^k \end{bmatrix} \times \begin{bmatrix} E_1^{k*} \\ E_2^{k*} \end{bmatrix} \right\rangle$$

$$= \begin{bmatrix} \langle E_1^k E_1^{k*} \rangle \\ \langle E_1^k E_2^{k*} \rangle \\ \langle E_2^k E_1^{k*} \rangle \\ \langle E_2^k E_2^{k*} \rangle \end{bmatrix} = \begin{bmatrix} J_{11}^k \\ J_{12}^k \\ J_{21}^k \\ J_{22}^k \end{bmatrix} \tag{10}$$

where $\times$ denotes the Kronecker product.
If Q is defined by

$$Q = \begin{bmatrix} 1 & 0 & 0 & 1 \\ 1 & 0 & 0 & -1 \\ 0 & 1 & 1 & 0 \\ 1 & -i & i & 0 \end{bmatrix} \tag{11}$$

the Stokes vector G is related to the coherency vector J by

$$G^k = QJ^k \ (k=i, f) \tag{12}$$

The coherency vector for the scattered waves is given by

$$\begin{aligned} J^f &= \langle E^f \times E^{f*} \rangle = \langle SE^i \times S^* E^{i*} \rangle \\ &= \langle (S \times S^*)(E^i \times E^{i*}) \rangle \\ &= \langle S \times S^* \rangle \langle E^i \times E^{i*} \rangle = \langle S \times S^* \rangle J^i \end{aligned} \tag{13}$$

Thus,

$$\begin{aligned} G^f &= QJ^f = Q \langle S \times S^* \rangle J^i \\ &= Q \langle S \times S^* \rangle Q^{-1} G^i = MG^i \end{aligned} \tag{14}$$

M is called the Mueller matrix and relates the incident Stokes vector to the scattered Stokes vector.

The elements of the Mueller matrix are

$$M = Q \begin{bmatrix} \langle S^{VV} S^{VV*} \rangle & \langle S^{VV} S^{VH*} \rangle & \langle S^{VH} S^{VV*} \rangle & \langle S^{VH} S^{VH*} \rangle \\ \langle S^{VV} S^{HV*} \rangle & \langle S^{VV} S^{HH*} \rangle & \langle S^{VH} S^{HV*} \rangle & \langle S^{VH} S^{HH*} \rangle \\ \langle S^{HV} S^{VV*} \rangle & \langle S^{HV} S^{VH*} \rangle & \langle S^{HH} S^{VV*} \rangle & \langle S^{HH} S^{VH*} \rangle \\ \langle S^{HV} S^{HV*} \rangle & \langle S^{HV} S^{HH*} \rangle & \langle S^{HH} S^{HV*} \rangle & \langle S^{HH} S^{HH*} \rangle \end{bmatrix} Q^{-1}$$

$$= [\,|A|B|C|D\,] \tag{15}$$

where

$$A = \begin{bmatrix} M_{11} \\ M_{21} \\ M_{31} \\ M_{41} \end{bmatrix}$$

$$= \begin{bmatrix} \frac{1}{2} \langle S^{VV} S^{VV*} + S^{VH} S^{VH*} + S^{HV} S^{HV*} + S^{HH} S^{HH*} \rangle \\ \frac{1}{2} \langle S^{VV} S^{VV*} + S^{VH} S^{VH*} - S^{HV} S^{HV*} - S^{HH} S^{HH*} \rangle \\ \langle \mathrm{Re}(S^{VV} S^{HV*} + S^{VH} S^{HH*}) \rangle \\ \langle \mathrm{Im}(S^{VV} S^{HV*} + S^{VH} S^{HH*}) \rangle \end{bmatrix} \tag{16}$$

$$B = \begin{bmatrix} M_{12} \\ M_{22} \\ M_{32} \\ M_{42} \end{bmatrix}$$

$$= \begin{bmatrix} \frac{1}{2} \langle S^{VV} S^{VV*} - S^{VH} S^{VH*} + S^{HV} S^{HV*} - S^{HH} S^{HH*} \rangle \\ \frac{1}{2} \langle S^{VV} S^{VV*} - S^{VH} S^{VH*} - S^{HV} S^{HV*} + S^{HH} S^{HH*} \rangle \\ \langle \mathrm{Re}(S^{VV} S^{HV*} - S^{VH} S^{HH*}) \rangle \\ \langle \mathrm{Im}(S^{VV} S^{HV*} + S^{VH*} S^{HH}) \rangle \end{bmatrix} \tag{17}$$

$$C = \begin{bmatrix} M_{13} \\ M_{23} \\ M_{33} \\ M_{43} \end{bmatrix}$$

$$= \begin{bmatrix} <\mathrm{Re}(S^{VV} S^{VH*} + S^{HV} S^{HH*})> \\ <\mathrm{Re}(S^{VV} S^{VH*} - S^{HV} S^{HH*})> \\ <\mathrm{Re}(S^{VV} S^{HH*} + S^{VH} S^{HV*})> \\ <\mathrm{Im}(S^{VV} S^{HH*} + S^{VH} S^{HV*})> \end{bmatrix} \quad (18)$$

and

$$D = \begin{bmatrix} M_{14} \\ M_{24} \\ M_{34} \\ M_{44} \end{bmatrix}$$

$$= \begin{bmatrix} <\mathrm{Im}(S^{VV*} S^{VH} + S^{HV*} S^{HH})> \\ <\mathrm{Im}(S^{VV*} S^{VH} + S^{HV} S^{HH*})> \\ <\mathrm{Im}(S^{VV*} S^{HH} + S^{VH} S^{HV*})> \\ <\mathrm{Re}(S^{VV} S^{HH*} - S^{VH} S^{HV*})> \end{bmatrix} \quad (19)$$

The Stokes vector G is related to the modified Stokes vector as follows

$$G = \begin{bmatrix} G_0 \\ G_1 \\ G_2 \\ G_3 \end{bmatrix} = \begin{bmatrix} <|E_1|^2+|E_2|^2> \\ <|E_1|^2-|E_2|^2> \\ 2\mathrm{Re} <E_1 E_2^*> \\ 2\mathrm{Im} <E_1 E_2^*> \end{bmatrix}$$

$$= \begin{bmatrix} 1 & 1 & 0 & 0 \\ 1 & -1 & 0 & 0 \\ 0 & 0 & 1 & 0 \\ 0 & 0 & 0 & 1 \end{bmatrix} \begin{bmatrix} <|E_1|^2> \\ <|E_2|^2> \\ 2\mathrm{Re}<E_1 E_2^*> \\ 2\mathrm{Im}<E_1 E_2^*> \end{bmatrix}$$

$$= \mathrm{N} G_m \quad (20)$$

Substituting this relationship in (14) leads to

$$\mathrm{N} G_m^f = \mathrm{MN} G_m^i = \mathrm{Q} <\mathrm{S} \times \mathrm{S}^*> \mathrm{Q}^{-1} \mathrm{N} G_m^i \quad (21)$$

Thus, the modified Mueller matrix M_m is given by

$$\mathrm{M}_m = \mathrm{N}^{-1}\mathrm{MN} = \mathrm{N}^{-1} \mathrm{Q} <\mathrm{S} \times \mathrm{S}^*> \mathrm{Q}^{-1} \mathrm{N}$$
$$= [|A_m| \ |B_m| \ |C_m| \ |D_m] \quad (22)$$

where

$$A_m \begin{bmatrix} M_{m11} \\ M_{m21} \\ M_{m31} \\ M_{m41} \end{bmatrix} = \begin{bmatrix} <S^{VV} S^{VV*}> \\ <S^{HV} S^{HV*}> \\ <2\mathrm{Re}\ (S^{VV} S^{HV*})> \\ <2\mathrm{Im}\ (S^{VV} S^{HV*})> \end{bmatrix} \quad (23)$$

$$B_m \begin{bmatrix} M_{m12} \\ M_{m22} \\ M_{m32} \\ M_{m42} \end{bmatrix} = \begin{bmatrix} <S^{VH} S^{VH*}> \\ <S^{HH} S^{HH*}> \\ <2\mathrm{Re}\ (S^{VH*} S^{HH})> \\ <2\mathrm{Im}\ (S^{VH} S^{HH*})> \end{bmatrix} \quad (24)$$

$$C_m \begin{bmatrix} M_{m13} \\ M_{m23} \\ M_{m33} \\ M_{m43} \end{bmatrix}$$

$$= \begin{bmatrix} <\mathrm{Re}(S^{VV} S^{VH*})> \\ <\mathrm{Re}(S^{HV} S^{HH*})> \\ <\mathrm{Re}(S^{VH*} S^{HV} + S^{VV} S^{HH*})> \\ <\mathrm{Im}(S^{VH} S^{HV*} + S^{VV} S^{HH*})> \end{bmatrix} \quad (25)$$

and

$$D_m \begin{bmatrix} M_{m14} \\ M_{m24} \\ M_{m34} \\ M_{m44} \end{bmatrix}$$

$$= \begin{bmatrix} -<\mathrm{Im}(S^{VV} S^{VH*})> \\ -<\mathrm{Im}(S^{HV} S^{HH*})> \\ -<\mathrm{Im}(S^{VH*} S^{HV} + S^{VV} S^{HH*})> \\ <\mathrm{Re}(S^{VV} S^{HH*} - S^{VH} S^{HV*})> \end{bmatrix} \quad (26)$$

Based on the definition

$$S^{PQ} = G_0 S_0^{PQ}$$
$$= G_0 \iint D^{PQ} [\exp(i\bar{v} \cdot \bar{r}_s) - \exp(\bar{iv} \cdot \bar{r}_t)] dx_s\, dz_s \quad (27)$$

the quantity $<S^{PQ}\ S^{RS*}>_{in}$ is defined in a manner analogous to the definition of the incoherent scattering cross section as

$$<S^{PQ}\ S^{RS*}>_{in} = \frac{4\pi^2}{A_y} [<S^{PQ}\ S^{RS*}> - <S^{PQ}><S^{RS*}>] \quad (28)$$

Unless otherwise mentioned, the operator $<\ >$ in the Mueller matrix (15) and the modified Mueller matrix (22) denotes incoherent averaging (28).

For the assumed isotropic random rough surfaces, the full wave expression for $<S^{PQ}\ S^{RS*}>_{in}$ can be shown to be given by[9], [10]

$$<S^{PQ}\ S^{PQ*}>_{in} = \frac{k_0^4}{\pi v_y^2} \cdot 2\pi$$
$$\times \iiint f_{RS}^{PQ}(\bar{n}) \{|\chi(v_y)|^2 [\exp(\frac{\sigma_s^2}{2} v_y^2 r_d^2 \exp(-\frac{2r_d^2}{l_c^2})$$
$$+ <h^2> v_y^2 \exp(-\frac{r_d^2}{l_c^2})) J_0(v'_{xz} r_d) - J_0(v_{xz} r_d)]$$
$$- \chi(v_y) [\exp(\frac{\sigma_s^2}{2} v_y^2 r_d^2 \exp(-\frac{2r_d^2}{l_c^2})) J_0(v'_{xz} r_d)$$
$$- J_0(v_{xz} r_d)]\} P(h_x, h_z)\ r_d\, dr_d\, dh_x\, dh_z \quad (29)$$

where

$$f_{RS}^{PQ}(\bar{n}) = D^{PQ}(\bar{n}) D^{RS*}(\bar{n}) P_2(\bar{n}', \bar{n}'|\bar{n}) \quad (30a)$$

$$v_{xz} = \sqrt{v_x^2 + v_z^2},\ v'_{xz} = \sqrt{(v'_x)^2 + (v'_z)^2} \quad (30b)$$

$$v'_x = v_x + v_y h_x \exp(-\frac{r_d^2}{4l_c^2}) \quad (30c)$$

$$v'_z = v_z + v_y h_z \exp(-\frac{r_d^2}{4l_c^2}) \quad (30d)$$

In (29), $P(h_x, h_z)$ is the probability density function for the surface slopes in x and z directions (assumed here to be Gaussian), $\bar{n}$ is the unit vector normal to the rough surface, P_2 is Saucer's shadow function[13], χ is the surface height characteristic function, $<h^2>$ and σ_s^2 are the mean square height and slope, l_c is the surface correlation length, and r_d is the distance variable[8][9].

2-3 Ellipsometric parameters

The ellipsometric parameters Ψ and Δ are defined as follows [Azzam and Bashara, 1977]

$$\frac{S^{VV}}{S^{HH}} = \frac{|S^{VV}|\exp(i\phi^{VV})}{|S^{HH}|\exp(i\phi^{HH})}$$
$$= \left|\frac{S^{VV}}{S^{HH}}\right| \exp[i(\phi_{VV} - \phi_{HH})]$$
$$= \tan(\Psi)\exp(i\Delta) \quad (31)$$

We immediately see that they are related to the Mueller matrix elements as follows

$$\Psi = \tan^{-1}\left(\sqrt{\frac{<S^{VV}\ S^{VV*}>}{<S^{HH}\ S^{HH*}>}}\right)$$
$$= \tan^{-1}\left(\sqrt{\frac{M_{m11}}{M_{m22}}}\right) \quad (32)$$

and

$$\tan(\Delta) = \frac{\sin(\Delta)}{\cos(\Delta)}$$

$$= \frac{\mathrm{Im}(<S^{VV}\,S^{HH*}>)}{\mathrm{Re}(<S^{VV}\,S^{HH*}>)} = \frac{M_{34}-M_{43}}{M_{33}+M_{44}} \qquad (33)$$

Thus

$$\Delta = \tan^{-1}\left(\frac{M_{34}-M_{43}}{M_{33}+M_{44}}\right) \qquad (34)$$

The ellipsometric parameters Ψ and Δ are also associated with ellipticity χ and orientation (see Fig. 1) by

$$\tan\chi = \frac{b}{a} \qquad (33)$$

$$\tan 2\alpha = \tan 2\Psi \cos\Delta \qquad (34)$$

and

$$\cos 2\chi = \frac{\cos 2\Psi}{\cos 2a} = \frac{\sin 2\Psi \cos\Delta}{\sin 2a} \qquad (35)$$

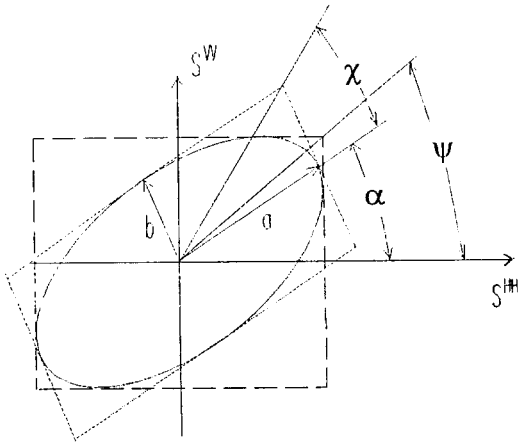

Fig. 1. Ellipsometric parameters.

Ⅲ. Illustrative examples

In the following illustrative examples, the scatter wave vector is the negative of the incident wave vector ($\bar{k}_0^f = -\bar{k}_0^i$). The remote sensing problems are usually related to the scattering in this backscatter direction only. The mean square slope is a fixed quantity $\sigma_{sT}^2 = 0.01$ (for Fig. 2 through 6) or $\sigma_{sT}^2 = 0.36$ (for Fig. 7 through 11). The root mean square height and the correlation length are gradually increased keeping the mean square slope constant. This results in a gradual increase of the surface radii of curvature.

For the three cases of surface roughness specified in Table 3, the modified Mueller matrix elements M_{m11} (Fig. 2), M_{m22} (Fig. 3), M_{m33} (Fig. 4), M_{m12} (Fig. 5), and M_{m34} (Fig. 6) in the backscatter direction are plotted as a function of incident angle.

Table 3. Surface roughness parameters (with a fixed mean square slope σ_{sT}^2=0.01) for Figures 2, 3, 4, 5, and 6 (Modified Mueller matrix in backscatter directions)

kh	kl_c	σ_{sT}^2	ε_r
0.05	1.0	0.01	5-i0.07
0.1	2.0	0.01	5-i0.07
0.2	4.0	0.01	5-i0.07

In Fig. 2 and 3, M_{m11} and M_{m22} are plotted for θ_0^i=0°~90°, respectively. M_{m11} and M_{m22} correspond to the like-polarized scattering cross sections $<\sigma_I^{VV}>$ and $<\sigma_I^{HH}>$ (see (23) and (24)). The surfaces with small root mean square heights (kh=0.05 and 0.1) are shown to give much smaller radar returns than the surface with the large rms height kh=0.2. In any of these cases, if the incident angle is beyond

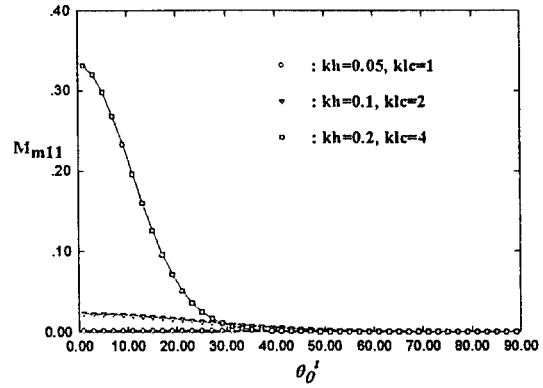

Fig. 2. Modified Mueller matrix element M_{m11} for σ_{ST}^2=0.01 in the backscatter direction, ε_r =5-i0.07.

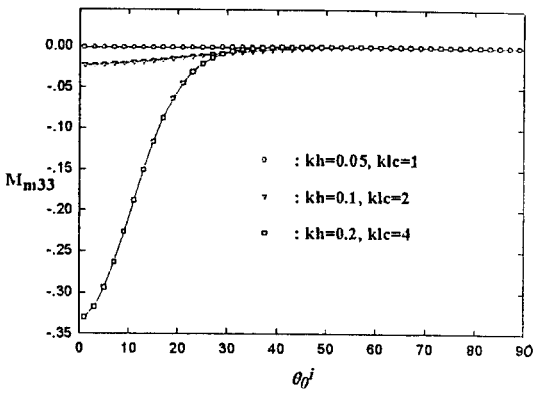

Fig. 4. Modified Mueller matrix element M_{m33} for σ_{ST}^2=0.01 in the backsatter direction, ε_r =5-i0.07.

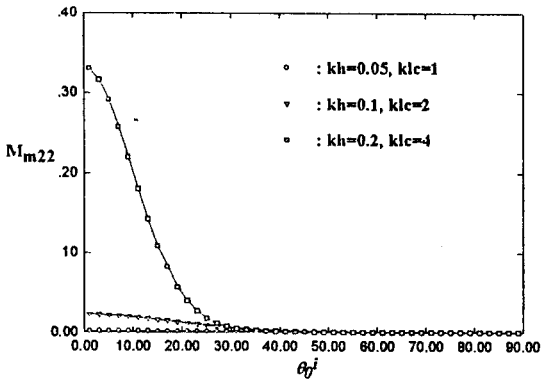

Fig. 3. Modified Mueller matrix element M_{m22} for σ_{ST}^2=0.01 in the backscatter direction, ε_r =5-i0.07.

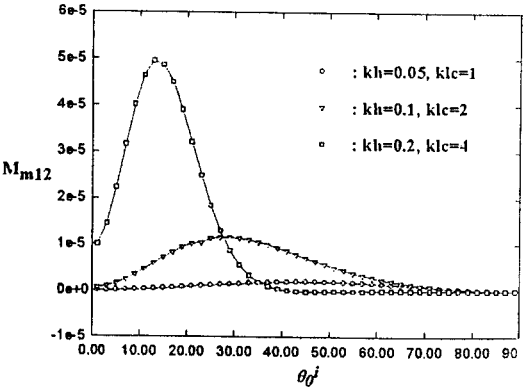

Fig. 5. Modified Mueller matrix element M_{m12} for σ_{ST}^2=0.01 in the backsatter direction, ε_r =5-i0.07.

30°, the radar returns of the scattered waves are very small. We also see that for this case, there is no particular difference between the scattering patterns for the two polarizations (*V-V* and *H-H*). M_{m33}(see (25)) in Fig. 4 is mainly related with the cosines of the phase difference between S^{VV} and S^{HH} because the order of $|S^{PQ}|(P\neq Q)$ is usually $10^{-2}\sim10^{-3}$ of $|S^{PQ}|$ $(P=Q)$. For small slope surfaces as given by this example, $|S^{VV}|\cong|S^{HH}|$ and they are 180° out of phase. This is why M_{m33} looks to be almost similar to the negative of M_{m11} (or M_{m22}).

In Fig. 5, M_{m12} is plotted for θ_0^i=0°~90°. M_{m12} is the same as the cross-polarized scattering cross sections $<\sigma_I^{VH}>$ (see (24)). For scat-

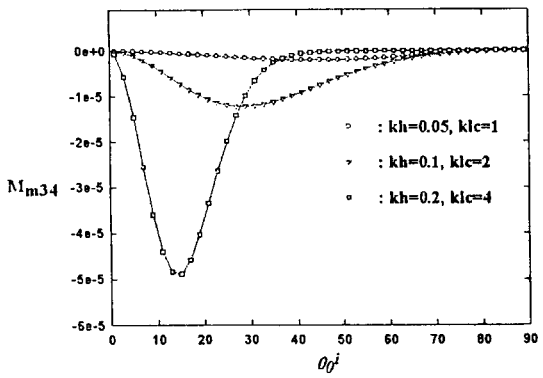

Fig. 6. Modified Mueller matrix element M_{m34} for σ_{sT}^2=0.01 in the backscatter direction, ε_r=5-i0.07.

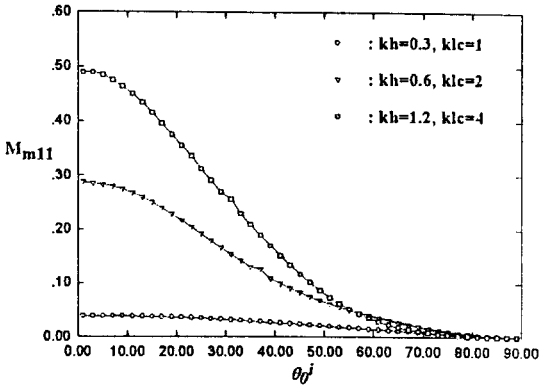

Fig. 7. Modified Mueller matrix element M_{m11} for σ_{sT}^2=0.36 in the backscatter direction, ε_r=5-i0.07.

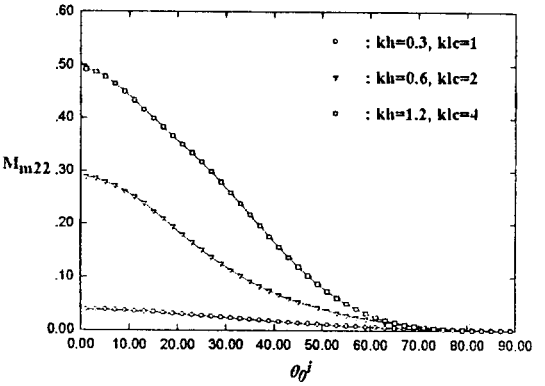

Fig. 8. Modified Mueller matrix element M_{m22} for σ_{sT}^2=0.36 in the backscatter direction, ε_r=5-i0.07.

tering in the backscatter direction, $M_{m12} = M_{m21}$. What is immediately noticed is that at near normal incidence (up to θ_0^i=27°) M_{m12} is larger for the cases with larger rms height. These three cases have peaks at θ_0^i=13° (the third case), 29° (the second case), and 51° (the first case), respectively. Fig. 6 shows that at normal incidence M_{m34} almost vanishes. This is clear when we check the expression M_{m34} in (26). The second term dominates over the first term and the second term is related to the sines of the relative phase difference between S^{VV} and S^{HH}, which go to zero at normal incidence.

In the next set of illustrative examples, the mean square slope is again a fixed quantity but it is increased to σ_{sT}^2=0.36. The root mean square height and the correlation length are gradually increased keeping the mean square slopes constant. The modified Mueller matrix elements M_{m11} (Fig. 7), M_{m22} (Fig. 8), M_{m33} (Fig. 9), M_{m12} (Fig. 10), and M_{m34} (Fig. 11) in the backscatter direction are plotted as a function of incident angle for the three cases of surface roughness given in Table 4.

In Fig. 7 and 8, we see that as the root mean square height becomes larger, M_{m11} and M_{m22} become larger. The levels of these cases considered here (σ_{sT}^2 =0.36) are all higher than the cases considered in Figures 2 and 3 (σ_{sT}^2 =0.01). The results also show that for sur-

Table 4. Surface roughness parameters (with a fixed mean square slope σ_{sT}^2=0.36) for Fig. 7, 8, 9, 10, and 11 (Modified Mueller matrix in backscatter directions)

kh	kl_c	σ_{sT}^2	ε_r
0.3	1.0	0.36	5-i0.07
0.6	2.0	0.36	5-i0.07
1.2	4.0	0.36	5-i0.07

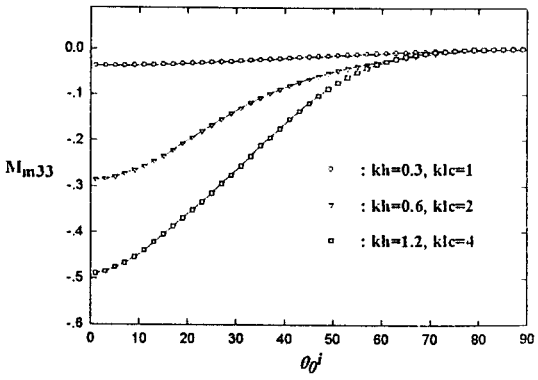

Fig. 9. Modified Mueller matrix element M_{m33} for σ_{sT}^2=0.36 in the backscatter direction, ε_r=5-i0.07.

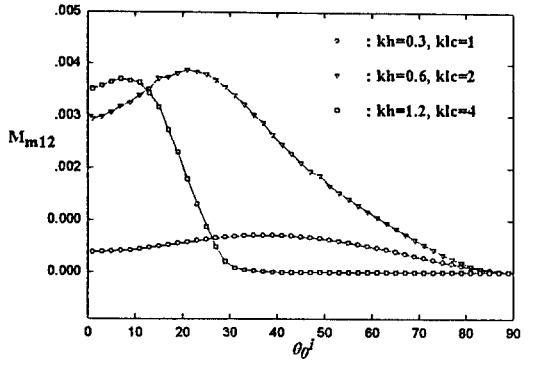

Fig. 10. Modified Mueller matrix element M_{m12} for σ_{sT}^2=0.36 in the backscatter direction, ε_r=5-i0.07.

faces with larger mean square slopes (σ_{sT}^2=0.36), significant radar returns can be obtained if the incident angle is less than θ_0^i=60° as compared to 30° (Fig. 2 and 3).

M_{m33} in Fig. 9 shows similar results to those in Fig. 4. However, the levels in this case are larger.

Fig. 10 shows that at near normal incidence, M_{m12} is largest for the third case (kh=1.2, kl_c=4) but it becomes smaller than M_{m12} for the second case (kh=0.6, kl_c=2) beyond the crossover angle θ_0^i=13°. What is interesting about the plots in Fig. 11 is that M_{m34} for the third case (kh=1.2, kl_c=4) goes through a fluctuation in sign as the incident angles become larger than 20°. The crossover in sign occurs as the phase difference between S^{VV} and S^{HH} becomes exactly 180° as for near normal incidence. These fluctuations in the relative phase is more pronounced as the rms height increases.

In the next set of examples, the incident angle is fixed at θ_0^i = 20° and the modified Mueller matrix elements in the backscatter di-

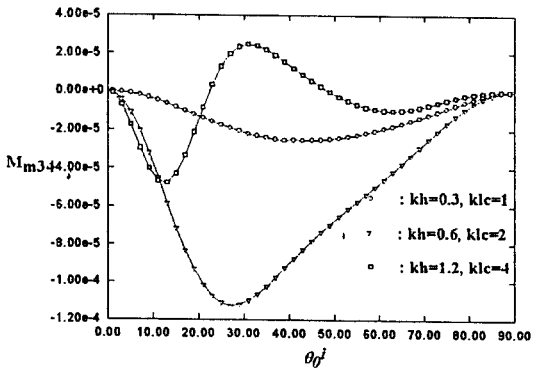

Fig. 11. Modified Mueller matrix element M_{m34} for σ_{sT}^2=0.36 in the backscatter direction, ε_r=5-i0.07.

rection are plotted as a function of surface height ($0 \le kh \le 0.35$) and correlation length ($1 \le kl_c \le 10$).

In Fig. 12, it is shown that M_{m11} increases as kh increases. For the surfaces with small slopes (large kl_c and small kh), M_{m11} is negligibly small because the waves are reflected mostly in the specular direction, not in the backscatter direction. For a fixed root mean square height kh, M_{m11} is largest when $kl_c \approx 3$. M_{m22} in Fig. 13 shows similar results to M_{m11} except that its magnitudes are smaller. In Fig. 14, the M_{m33} is shown to be similar to the negative of M_{m11}(or M_{m22}). This is because that for the incident angle $\theta_0^i = 20°$, $|S^{VV}| \cong |S^{HH}|$, and they are 180° out of phase (see (25)). In the expression for M_{m33}, the second term is more important than the first one since $|S^{PQ}|$ $(P \neq Q)$ is $10^{-2} \sim 10^{-3}$ of $|S^{PQ}|$ $(P=Q)$ in most cases.

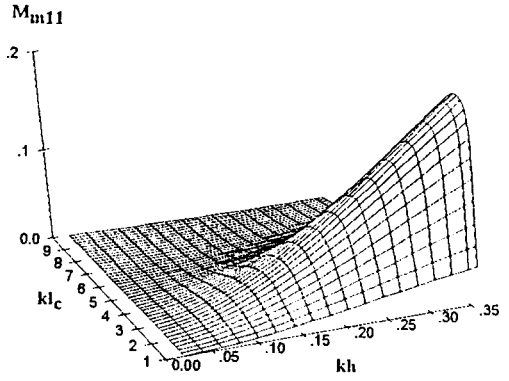

Fig. 12. Modified Mueller matrix element M_{m11} in the backscatter direction with $\theta_0^i = 20°$, as a function of kh and kl_c, ε_r=5-i0.07.

M_{m12} in Fig. 15 shows the depolarization tendency of the horizontally polarized waves to

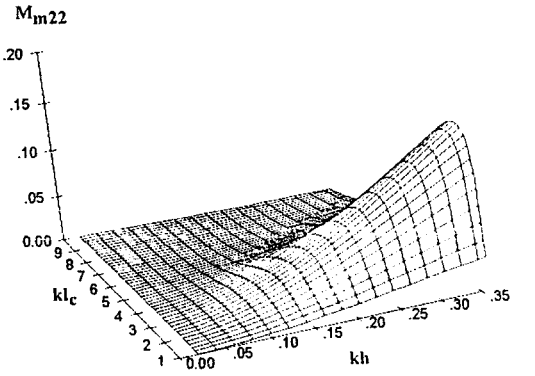

Fig. 13. Modified Mueller matrix element M_{m22} in the backscatter direction with $\theta_0^i = 20°$, as a function of kh and kl_c, ε_r=5-i0.07.

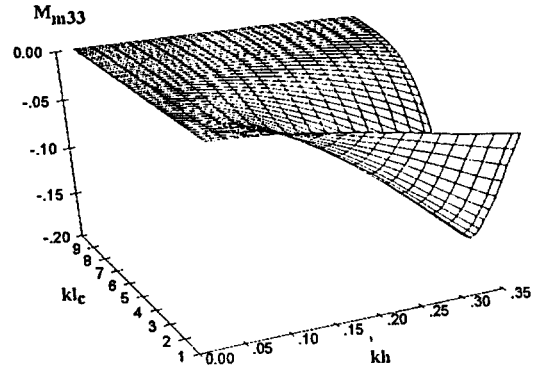

Fig. 14. Modified Mueller matrix element M_{m33} in the backscatter direction with $\theta_0^i = 20°$, as a function of kh and kl_c, ε_r=5-i0.07.

the vertically polarized waves. M_{m12} is shown to increase as kh, increases. For a fixed root mean square height kh, M_{m12} is largest when $kl_c \approx 2$. Its levels are about 20 dB less than in the like-polarized cases given in Fig. 12 and 13. In Fig. 16, M_{m34} decreases as kh increases. For a fixed root mean square height kh, M_{m34} is smallest when $kl_c \approx 3$.

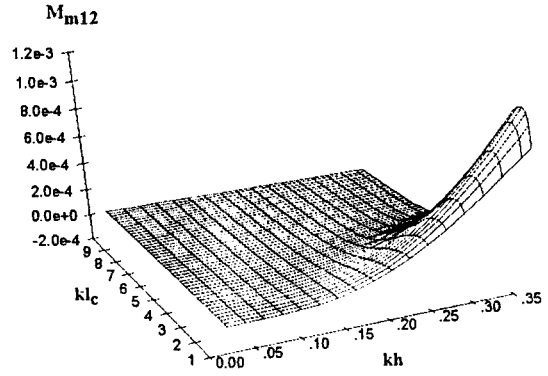

Fig. 15. Modified Mueller matrix element M_{m12} in the backscatter direction with θ_0^i=20°, as a function of kh and kl_c, ε_r=5-i0.07.

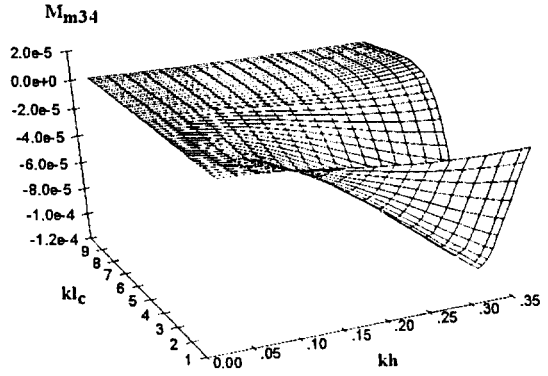

Fig. 16. Modified Mueller matrix element M_{m34} in the backscatter direction with θ_0^i=20°, as a function of kh and kl_c, ε_r=5-i0.07.

In the following illustrative examples, we plot the Stokes vector elements of the scattered waves as a function of the ellipsometric parameters Ψ and Δ (in this case $\Delta=\phi$) of the incident waves as follows

$$\begin{bmatrix} G_0^f \\ G_1^f \\ G_2^f \\ G_3^f \end{bmatrix} = \mathrm{M} \begin{bmatrix} |E_1^i|^2 + |E_2^i|^2 \\ |E_1^i|^2 + |E_2^i|^2 \\ 2|E_1^i||E_2^i| \cos\phi \\ 2|E_1^i||E_2^i| \sin\phi \end{bmatrix}$$

$$= \mathrm{M} \begin{bmatrix} \sin^2\Psi + \cos^2\Psi \\ \sin^2\Psi - \cos^2\Psi \\ 2\cos\Psi \sin\Psi \cos\Delta \\ 2\cos\Psi \sin\Psi \sin\Delta \end{bmatrix} \tag{36}$$

$$= \mathrm{M} \begin{bmatrix} 1 \\ -\cos 2\Psi \\ \sin 2\Psi \cos\Delta \\ \sin 2\Psi \sin\Delta \end{bmatrix}$$

The incident wave is completely polarized ($G_0^2=G_1^2+G_2^2+G_3^2$) and its total power is chosen to be 1. M is the Mueller matrix. The surface roughness parameters considered here are kh=0.6, kl_c=2, and ε_r=5-i0.07. The incident angle is θ_0^i=60° and the scatter angle is in the backscatter direction . For this specific case, M is computed to be

$$\mathrm{M}=\begin{bmatrix} 0.29825\times10^{-1} & 0.86670\times10^{-2} & 0 & 0 \\ 0.86670\times10^{-2} & 0.27593\times10^{-1} & 0 & 0 \\ 0 & 0 & -0.27336\times10^{-1} & -0.47841\times10^{-4} \\ 0 & 0 & 0.47841\times10^{-4} & -0.25100\times10^{-1} \end{bmatrix} \tag{37}$$

Note that the top right 2×2 elements and bottom left 2×2 elements vanish. The reason for this is that the scattering matrix coefficients S^{PQ} ($P=Q$) are even functions of the surface slopes h_x and h_z, and S^{PQ} ($P\neq Q$) are odd functions of the surface slopes h_x and h_z.

In Fig. 17, G_0^f is plotted. Ψ=90° corresponds to the vertically polarized incident waves and Ψ=0° corresponds to the horizontally polarized incident waves. This Figure tells that when the incident waves are vertically polarized, more radar returns are expected than when

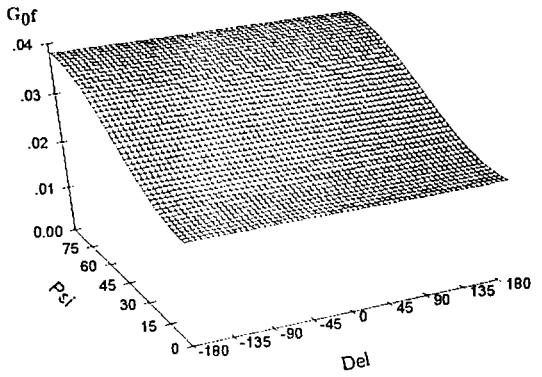

Fig. 17. Stokes vector element G_0^f based on ellipsometric parameters Ψ(Psi) and Δ (Del).
kh=0.6, kl_c=2, σ_{sT}^2=0.36, θ_0^i=60° (backscatter), ε_r=5-i0.07.

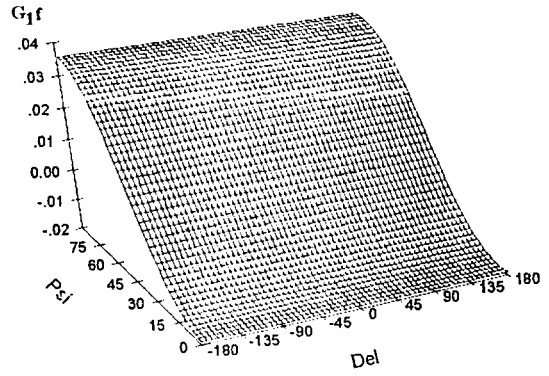

Fig. 18. Stokes vector element G_1^f based on ellipsometric parameters Ψ(Psi) and Δ (Del).
kh=0.6, kl_c=2, σ_{sT}^2=0.36, θ_0^i=60° (backscatter), ε_r=5-i0.07.

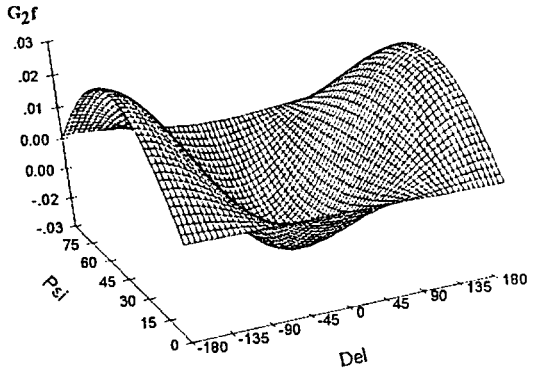

Fig. 19. Stokes vector element G_2^f based on ellipsometric parameters Ψ(Psi) and Δ (Del).
kh=0.6, kl_c=2, σ_{sT}^2=0.36, θ_0^i=60° (backscatter), ε_r=5-i0.07.

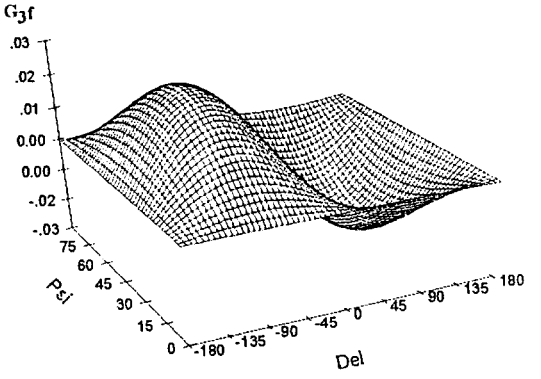

Fig. 20. Stokes vector element G_3^f based on ellipsometric parameters Ψ(Psi) and Δ (Del).
kh=0.6, kl_c=2, σ_{sT}^2=0.36, θ_0^i=60° (backscatter), ε_r=5-i0.07.

the incident waves are horizontally polarized, but they are insensitive to the variations of relative phase difference Δ. In Fig. 18, it is shown that the difference of the powers in vertical and horizontal polarizations of the scattered waves is also affected more by the vertically polarized incident waves than the horizontally polarized incident waves.

In Fig. 19, we see that while G_2^f is the cosine function of Δ when Ψ=45°, it is independent

of Δ when $\Psi=0°$ or $\Psi=90°$. In Fig. 20, we see that while G'_3 is the sine function of Δ when $\Psi=45°$, it is independent of Δ when $\Psi=0°$ or $\Psi=90°$.

Ⅲ. Conclusions

The various aspects of the Mueller matrix elements have been considered for a wide range of surface roughness (Fig. 2 through 11). The Stokes vector elements of the scattered wave have been investigated as a function of ellipsometric parameters of the incident wave (Fig. 17 through 20). For isotropic random rough surfaces, the top right 2×2 elements and bottom left 2×2 elements vanish. For scattering in the backscatter direction, $M_{12}=M_{21}$. Furthermore, since $|S^{pq}|(P\neq Q)$ is usually $10^{-2}\sim10^{-3}$ of $|S^{pq}|(P=Q)$, $M_{33}\approx M_{44}$ and $M_{34}\approx -M_{43}$. Thus, for scattering in the backscatter direction, the 5 elements (M_{m11}, M_{m22}, M_{m33}, M_{m12}, and M_{m34}) are practically important. The Mueller matrix data as given by the Fig. 12 through 16 may be used as a guide for remote sensing of rough surface characteristics or RCS problems.

Reference

[1] S. O. Rice, "Reflection of electromagnetic waves from slightly rough surface," *Commun. Pure Appl. Math., 4,* pp. 251-378, 1951.

[2] P. Beckmann, and A. Spizzichino, *The Scattering of Electromagnetic Waves From Rough Surface,* Macmillan, New York, 1963.

[3] G. S. Brown, "Backscattering from a Gaussian distributed perfectly conducting rough surface," *IEEE Trans. Antennas Propag., Ap-26*(3), pp. 472-482, 1978.

[4] M. Nieto-Vesperinas, and J. M. Soto-Crespo, "Monte Carlo simulations for scattering of electromagnetic waves from perfectly conductive random rough surfaces," *Optics Letters, 12*(12), pp. 979-981, 1987.

[5] J. A. Sanchez-Gil, and M. Nieto-Vesperinas, "Light scattering from random rough dielectric surfaces," *J. Opt. Soc. Am. A, 8*(8), pp. 1270-1286, 1991.

[6] E. Bahar, "Full wave analysis for rough surface diffuse, incoherent radar cross sections with height-slope correlatios included," *IEEE Trans. Antennas Propag., Ap-39*(9), pp. 1293-1304, 1991.

[7] E. Bahar, and B. S. Lee, "Full wave solutions for rough surface bistatic radar cross sections-Comparison with small perturbation, physical optics, numerical, and expermental results," *Radio Sci., 29*(2), pp. 407-429, 1994a.

[8] E. Bahar, and B. S. Lee, "Full wave vertically polarized bistatic radar cross sections for random rough surfaces-Comparison with experimental and numerical results," *IEEE Trans. Antennas Propag. 43* (2), pp. 205-213, 1995a.

[9] E. Bahar, and B. S. Lee, "Radar scatter cross sections for two-dimensional random rough surface-full wave solutions and comparisons with experiments," *Waves in Random Media,* No. 6, pp. 1-23, 1996.

[10] B. S. Lee and E. Bahar, "Mueller matrix associated wit diffuse sacttering from

two-dimensional random rough surfaces-Full wave analysis," *Proceedings of International Geoscience and Remote Sensing Symposium*, pp. 1794-1796, May 27-31, 1996.

[11] E. Bahar, "Full wave solutions for depolarization of the scattered radiation fields by rough surfaces of arbitrary slope," *IEEE Trans. Antennas Propag., Ap-29*(3), pp. 443-454, 1981a.

[12] H. Mott, *Antennas for Radar and Communications: A Polarimetric Approach*, John Wiley & Sons, New York, 1992.

[13] M. I. Sancer, "Shadow corrected electromagnetic scattering from randomly rough surface," *IEEE Trans. Antennas Propag., SP-17*, pp. 577-585, 1969.

[14] R. M. A. Azzam., and N. M. Bashara, *Ellipsometry and polarized Light*, North-Holland Publishing Company, Netherlands, 1977.

이 범 선

1958년 3월 26일생

1982년 2월 : 서울대학교 전기공학과 졸업 (학사)

1991년 8월 : 미국 네브래스카 주립대학 (석사)

1995년 5월 : 미국 네브래스카 주립대학 (박사)

1995년 5월~1995년 8월 : 미국 네브래스카 주립 대학 (Post-doctor)

1995년 9월~현재 : 경희대학교 전파공학과 조교수

[주 관심분야] 위상배열 안테나, 전파전파, 전자파 산란